

Sodium orthovanadate inhibits growth and triggers apoptosis of human anaplastic thyroid carcinoma cells *in vitro* and *in vivo*

QINGAN YU, WENJING JIANG, DAN LI, MINGQI GU, KUNPENG LIU,
LIQIAN DONG, CHAOQUN WANG, HONGCHI JIANG and WENJIE DAI

Department of General Surgery, The First Affiliated Hospital of Harbin Medical University,
Harbin, Heilongjiang 150001, P.R. China

Received May 3, 2018; Accepted December 17, 2018

DOI: 10.3892/ol.2019.10090

Abstract. Vanadium and its compounds exhibit concentration- and time-dependent anticancer effects on various types of tumor; however, the effects of sodium orthovanadate (SOV) on anaplastic thyroid carcinoma (ATC) have not yet been reported. In the present study, the anticancer effects of SOV on ATC were evaluated. *In vitro* experiments, including cell viability assays, plate colony formation assays, cell cycle analysis and apoptosis analysis were used to study the role of SOV in ATC. Using *in vivo* experiments, the effects of SOV on the growth and apoptosis of an ATC-xenograft tumor were studied by comparing the SOV-treatment with the control group. The results revealed that treatment of the human ATC cell line 8505C with SOV inhibited cell viability, induced G₂/M phase cell cycle arrest, stimulated apoptosis and reduced mitochondrial membrane potential in a concentration-dependent manner. These findings were confirmed *in vivo* in a nude mouse ATC xenograft model. In conclusion, the present study demonstrated that SOV inhibited human ATC by regulating proliferation, cell cycle progression and apoptosis, thus suggesting that SOV may be considered a novel option for the treatment of ATC.

Introduction

Anaplastic thyroid carcinoma (ATC) is a highly invasive, undifferentiated tumor characterized by rapid growth and distant metastasis. ATC accounts for <2% of all types of thyroid cancer, but is responsible for >50% of cases of thyroid cancer-associated mortality (1-3). Half of all cases of ATC-associated mortality are caused by upper airway

obstruction and asphyxia, whereas the remaining cases are attributed to local or distant metastases and/or treatment complications (4). The patient survival time after diagnosis is ~16 weeks, and the 1 and 5 year survival rates are 17 and 8%, respectively (5). In addition, the available treatments for ATC, including surgery, radiotherapy and chemotherapy, have poor results (6). Therefore, the development of novel approaches is crucial, and may include novel cytotoxic drugs, targeted molecular therapies and gene therapies, in order to kill ATC cells (7-10).

Vanadium is a transition metal that belongs to the group of micronutrients that are essential for normal metabolism. Notably, sodium orthovanadate (SOV) is a vanadium compound and phosphate analog, which possesses numerous biological activities, including inhibition of nonselective protein tyrosine phosphatases, alkaline phosphatases and ATPases, activation of tyrosine kinases, promotion of mitogenesis and neuroprotection, and inhibition of diabetic effects by an insulin-mimetic property (11,12). SOV can also inhibit the growth of central nervous system tumors (13), lung cancer (14), prostate cancer (15), bladder cancer (16) and liver cancer (17,18). However, the effects of SOV on ATC cells have not yet been reported.

The present study aimed to investigate the effects of SOV on ATC *in vitro* and *in vivo*. To do so, the influence of SOV on cell growth, cell cycle progression, apoptosis and mitochondrial membrane potential ($\Delta\psi_m$) were investigated.

Materials and methods

Cell culture, reagents and antibodies. The human ATC cell line 8505C was kindly provided by Dr Jihua Han (The Third Affiliated Hospital of Harbin Medical University, Harbin, China). Cells were cultivated in RPMI 1640 medium supplemented with 10% fetal bovine serum and 1% penicillin/streptomycin at 37°C in a humidified incubator containing 5% CO₂. SOV was purchased from Sigma-Aldrich (Merck KGaA, Darmstadt, Germany). Antibodies against Ki-67 (catalog no. 9449S) were provided by Cell Signaling Technology, Inc. (Danvers, MA, USA).

Cell viability assay. Cell viability was assessed with the Cell Counting kit-8 (CCK-8; Dojindo Molecular Technologies,

Correspondence to: Professor Hongchi Jiang or Professor Wenjie Dai, Department of General Surgery, The First Affiliated Hospital of Harbin Medical University, 23 Youzheng Street, Harbin, Heilongjiang 150001, P.R. China
E-mail: jianghc2013@163.com
E-mail: davidhmu@163.com

Key words: sodium orthovanadate, anaplastic thyroid carcinoma, 8505C cells, tumor growth, apoptosis

Inc., Kumamoto, Japan). Briefly, cells were cultured in 96-well plates with RPMI 1640 medium overnight prior to treatment with SOV (0, 0.5, 1, 2, 4 and 8 μM) for 1-6 days and incubated at 37°C. The cells were seeded between 500 and 3,000 cells/well, in 100 μl culture medium, depending on the culture times tested (1-6 days). After the appropriate culture time, 10 μl CCK-8 solution was added to each well for 1 h, prior to measuring the absorbance at 450 nm with a microplate reader. The half maximal inhibitory concentration (IC_{50}) values were calculated according to the Reed-Muench method (19). Experiments were performed three times.

Plate colony formation assay. Cells were seeded in 6-well plates at a density of 500 cells/well and incubated overnight at 37°C. They were then treated with various concentrations of SOV (0, 0.5, 1, 2, 4 and 8 μM) for 14 days and incubated at 37°C. Each treatment was carried out in triplicate. Plates were incubated for 14 days. Medium containing the appropriate concentration of SOV was replaced twice weekly. Eventually, plates were washed twice with cold PBS, fixed with 4% paraformaldehyde for 10 min, and stained with 3% crystal violet. Colonies containing ≥ 50 cells were scored.

Cell cycle analysis. Cell cycle progression of 8505C cells was analyzed using a Cell Cycle kit (catalog no. 558662; BD Biosciences, San Jose, CA, USA). Briefly, following treatment with various concentrations of SOV (0, 0.5, 1, 2, 4 and 8 μM) at 37°C for 48 h, cells were harvested. A total of 1×10^6 cells were incubated with reagents A-C, according to the manufacturer's protocol, and cells were subjected to flow cytometry. Experiments were performed three times.

Apoptosis analysis. Cell apoptosis was analyzed with the fluorescein isothiocyanate (FITC)/Annexin V Apoptosis Detection kit I (BD Biosciences), according to the manufacturer's protocol. Briefly, cells were treated with various concentrations of SOV (0, 2 and 4 μM) and incubated at 37°C for 48 h. Subsequently, cells were washed twice with cold PBS, resuspended in 1X Binding Buffer at a concentration of 1×10^6 cells/ml, and 100 μl of each cell solution was transferred to individual 5 ml culture tubes. A volume of 5 μl FITC-conjugated Annexin V and 5 μl propidium iodide were added to the tubes, which were gently vortex-mixed, prior to 15 min incubation in the dark at room temperature. A volume of 400 μl 1X Binding Buffer was then added to each tube. The samples were immediately analyzed by flow cytometry (<1 h). Experiments were performed three times.

$\Delta\psi\text{m}$ assessment. The lipophilic cationic dye JC-1 was used to measure alterations in $\Delta\psi\text{m}$. The JC-1 probe was provided by Beyotime Institute of Biotechnology (Haimen, China) and the assay was performed according to the manufacturer's protocol. Briefly, cells were incubated with SOV (0, 2 and 4 μM) in 6-well plates at 37°C for 48 h, prior to adding 5 $\mu\text{g}/\text{ml}$ JC-1 for 20 min at 37°C. After incubation with JC-1, cells were washed twice with PBS. The $\Delta\psi\text{m}$ was assessed by determining the dual emissions from mitochondrial JC-1 monomers (green, 490 nm stimulated luminescence and 530 nm emission light) and aggregates (red, 525 nm stimulated luminescence and 590 nm emission light) using a confocal laser scanning microscope. An

increase in the green/red fluorescence intensity ratio indicated mitochondrial depolarization. The relative $\Delta\psi\text{m}$ was calculated according to the following formula: Experimental ratio value/Control ratio value $\times 100$. Experiments were performed three times.

Xenograft tumor model and treatments. Female nude mice (5 weeks old; 16-18 g; Beijing Vital River Laboratories Animal Technology Co., Ltd., Beijing, China) were housed at a constant temperature (23°C) and relative humidity (60%) with a fixed 12-h light-dark cycle, and free access to food and water. After 1 week of feeding in the new environment, mice were then used to generate a subcutaneous tumor model. All surgical procedures and animal care protocols were approved by the Ethics Committee of the First Affiliated Hospital of Harbin Medical University (Harbin, China). The study also complied with institutional guidelines for animal care. An 8505C cell suspension (100 μl) in serum-free RPMI 1640 culture medium (1×10^6) was subcutaneously injected into the flanks of nude mice. Tumor formation and tumor size were monitored daily. When tumors were ~ 4 mm in diameter, animals were randomly divided into three groups, according to their similar average tumor sizes ($n=4$ mice/group). Mice received daily 200 μl intraperitoneal injections of either PBS (control) or SOV (5 or 10 mg/kg) in PBS. The doses and methods were based on our preliminary experiments and previous reports (17,20). Tumor size was assessed twice weekly at the skin surface and calculated as follows: Tumor volume=(width)² \times (length/2). After 4 weeks treatment, tumors were harvested, weighed and their volume was measured.

Detection of 8505C cell proliferation in vivo. Immuno histochemical analyses of the tumors were performed using an anti-Ki-67 antibody, in order to detect cancer cell proliferation. Briefly, tumor paraffin sections (4 μm) were prepared by fixation with 10% formaldehyde solution for 12 h at room temperature, washing with water for 24 h, dehydration, transparency, embedding with paraffin, sectioning and baking for 30 min at 60°C. Following dewaxing, rehydration and antigen retrieval, the tumor sections were blocked in 3% bovine serum albumin (catalog no. 37520; Thermo Fisher Scientific, Inc.) at room temperature for 2 h, and incubated overnight at 4°C with primary antibody against Ki-67 (1:200; catalog no. 8112S; Cell Signaling Technology, Inc.). Sections were subsequently incubated at room temperature for 30 min with SignalStain[®] Boost Detection Reagent (HRP, Mouse) (catalog no. 8125S; Cell Signaling Technology, Inc.), then examined by light microscopy (magnification, $\times 400$).

Detection of apoptosis of 8505C cells in vivo. Cell apoptosis was determined *in situ* with a terminal deoxynucleotidyl transferase dUTP nick-end labeling (TUNEL) cell apoptosis detection kit (Beyotime Institute of Biotechnology), according to the manufacturer's protocol. Briefly, 4 μm tumor sections were dewaxed with xylene twice for 5 min, and soaked in 100% ethanol for 5 min, 90% ethanol for 2 min and 70% ethanol for 2 min. Sections were rinsed with distilled water for 2 min and incubated with 20 $\mu\text{g}/\text{ml}$ proteinase K without DNase at 37°C for 15 min. They were eventually washed three times with PBS, and exposed to 50 μl TUNEL working fluid.

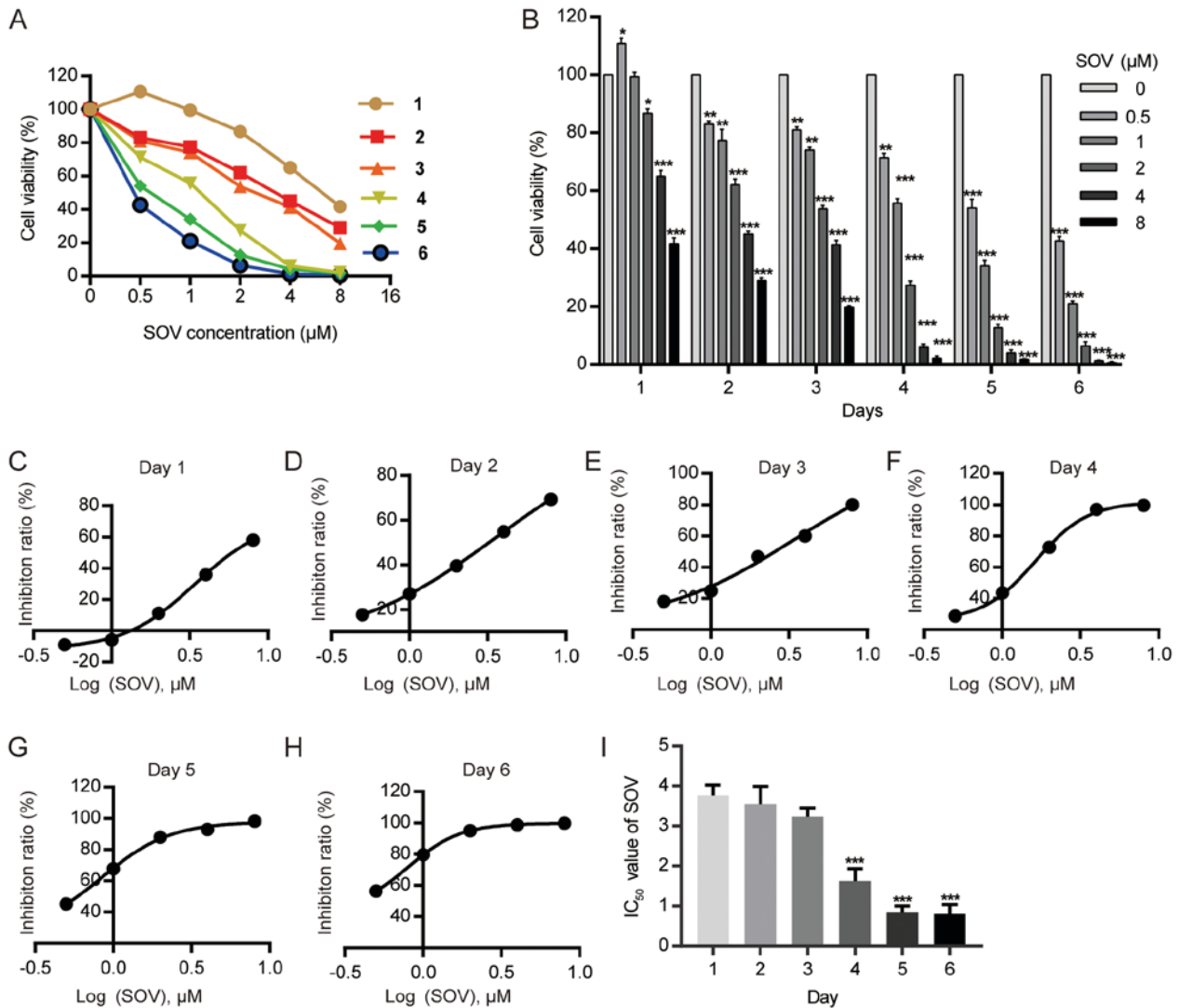


Figure 1. SOV inhibits 8505C cell growth in a dose- and time-dependent manner. (A and B) Viability index of 8505C cells treated with increasing concentrations of SOV for 1-6 days was determined using the Cell Counting kit-8 assay. * $P < 0.05$, ** $P < 0.01$, *** $P < 0.001$ vs. the control (0 μM SOV) group. (C-H) IC₅₀ curve following SOV treatment of 8505C cells for 1-6 days. (I) IC₅₀ values following SOV treatment of 8505C cells for 1-6 days. *** $P < 0.001$ vs. day 1. IC₅₀, half maximal inhibitory concentration; SOV, sodium orthovanadate.

A fluorescence microscope was used to capture images of 400 high-power fields from the slides. The apoptosis index (%) was calculated according to the following formula: Apoptosis index = Number of apoptotic cells / Total number of nucleated cells $\times 100$. Experiments were performed three times.

Statistical analysis. GraphPad Prism 7.0 (GraphPad Software, Inc., La Jolla, CA, USA) was used for statistical analysis. Data are expressed as the means \pm standard deviation. The differences among samples were evaluated by one-way analysis of variance followed by Dunnett's test. $P < 0.05$ was considered to indicate a statistically significant difference.

Results

Inhibitory effect of SOV on 8505C cell viability. The 8505C cell line was cultured with various concentrations of SOV (0.5, 1, 2, 4 and 8 μM) or without SOV (control group) for 1-6 days. The cell survival rate was determined using the CCK-8 kit (Fig. 1A). SOV inhibited the viability of 8505C

cells, and exhibited a stronger effect at higher concentrations (Fig. 1B). The IC₅₀ values of SOV for 8505C growth were 3.76, 3.55, 3.23, 1.62, 0.85 and 0.80 μM on days 1-6, respectively (Fig. 1C-I). The mean IC₅₀ was 2.30 μM .

SOV inhibits the clonogenic survival of 8505C cells. The effects of SOV on the clonogenic survival of 8505C cells were evaluated using colony formation assays. The 8505C cells were exposed to increasing concentrations of SOV (0.5, 1, 2, 4 and 8 μM) or culture medium for 14 days. A decrease in the number of ATC colonies following SOV treatment was observed in a concentration-dependent manner (Fig. 2A and B). Concentrations of SOV ≥ 1 μM inhibited $>50\%$ of 8505C cell colony formation compared with in the control group ($P < 0.01$), and 8 μM SOV inhibited 98% of the colony formation ($P < 0.001$).

SOV induces G₂M cell cycle arrest in 8505C cells. In order to explore the anti-proliferative mechanism of SOV, 8505C cell cycle progression was assessed following treatment with SOV.

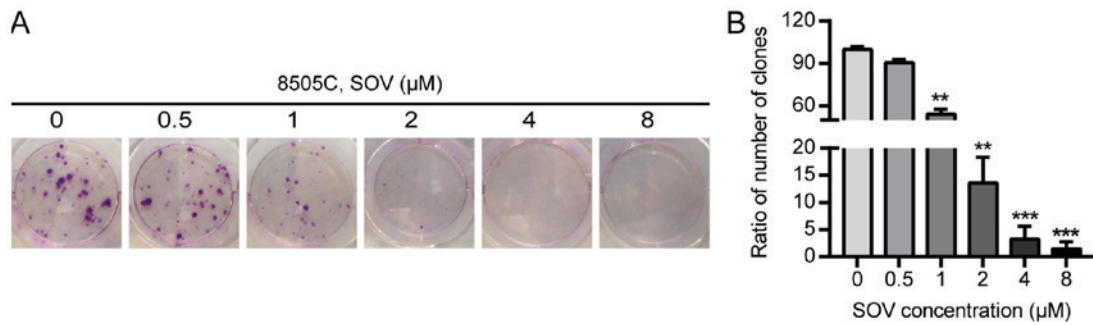


Figure 2. Colony formation of 8505C cells following SOV treatment for 14 days. (A) Colonies were stained with 3% crystal violet. (B) Rate of colony formation in response to each SOV concentration compared to that in the control group. ** $P < 0.01$, *** $P < 0.001$ vs. the control (0 μM SOV) group. SOV, sodium orthovanadate.

Briefly, 8505C cells were cultured in the presence of 0, 2 or 4 μM SOV, according to the mean IC_{50} for 48 h. Flow cytometric analysis revealed that SOV blocked the progression of 8505C cells beyond the G_2/M phase (Fig. 3A and B). Treatment with 4 μM SOV resulted in the accumulation of 40% of cells in the G_2/M phase, whereas only 10% of cells in the control group were in the G_2/M phase ($P < 0.001$). These data suggested that SOV may lead to G_2/M phase arrest in 8505C cells.

SOV induces apoptosis of 8505C cells. Following treatment with SOV for 48 h, the apoptotic rate of 8505C cells treated with SOV was significantly higher than that of the control group ($P < 0.01$, Fig. 4A and B). Treatment with 2 μM SOV for 48 h increased the percentage of apoptotic 8505C cells to 20%, and 4 μM SOV resulted in ~40% apoptotic cells. These data suggested that SOV may induce 8505C cell apoptosis in a concentration-dependent manner.

SOV diminishes the $\Delta\psi\text{m}$ of 8505C cells. The effects of SOV on $\Delta\psi\text{m}$ were then assessed. The 8505C cells treated with 2 or 4 μM SOV for 48 h exhibited lower red and higher green fluorescence than those of the control group, and $\Delta\psi\text{m}$ alterations were observed in a concentration-dependent manner (Fig. 5A). In addition, 60 and 80% of cells exhibited green fluorescence (early apoptotic) in the groups treated with 2 and 4 μM , respectively (Fig. 5B).

SOV inhibits xenograft tumor growth and induces apoptosis in vivo. Following treatment of nude mice with SOV, or PBS as a control, tumor volume was calculated by assessing tumor diameter weekly. The results demonstrated that the tumor volume in the SOV group was smaller than that in the control group from the first week, and the difference in tumor volume between groups was positively associated with treatment duration. In the two SOV intervention groups, the tumor volume in the high-concentration group (10 mg/kg) was smaller than that in the low-concentration group (5 mg/kg; $P < 0.05$, Fig. 6A and B). This suggested that treatment with SOV significantly inhibited tumor growth compared to that in the control group. Therefore, SOV may inhibit the growth of ectopic ATC.

In order to detect 8505C cell proliferation after SOV or PBS treatment, the expression of the proliferative biomarker protein Ki-67 was detected by immunohistochemistry. The results

revealed that the expression of Ki-67 in the tumor tissues of the SOV group was significantly lower than that in the control group. In addition, Ki-67 expression in the high-SOV group (10 mg/kg) was significantly lower than that in the low-SOV group (5 mg/kg; $P < 0.05$, Fig. 6C and D). In order to assess the apoptosis of 8505C cells, an *in situ* TUNEL assay was performed. The results demonstrated that the number of apoptotic cells treated with SOV was higher than that in the control group, and was positively associated with SOV concentration (Fig. 6E and F). These results revealed that SOV inhibited the proliferation and promoted the apoptosis of 8505C cells *in vivo*.

Discussion

ATC is the most malignant type of thyroid cancer, and is characterized by early metastasis and invasion of local organs. Surgical treatment commonly fails as a radical treatment. To the best of our knowledge, there is currently no efficient chemotherapeutic drug able to control ATC development. It is therefore crucial to develop novel treatments. In the present study, SOV promoted the apoptosis of 8505C cells, leading to G_2/M phase cell cycle arrest. These results provided a novel option for the treatment of undifferentiated thyroid cancer.

Previous studies have revealed that vanadium salts can inhibit the progression of various tumors and trigger apoptosis of numerous cancer cells, including neuroblastoma (SH-SY5Y cells) (13), lung cancer (A549 cells) (14), renal cancer (HTB44 cells) (14), prostate cancer (DU145 and PC-3 cells) (14,15), bladder cancer (T24 cells) (16), liver cancer (HepG2, SK-Hep-1, Hep3B and h35-19 cells) (17,18) and monocytic leukemia (U937 cells) (21). Nevertheless, some studies revealed that vanadium salts can promote tumor progression. For instance, Afshari *et al* demonstrated that vanadium salts cause Syrian hamster embryo cells to escape senescence and become immortalized at a low frequency, eventually leading to the occurrence of tumors (22). In addition, Hwang *et al* reported that vanadium salts lead to tumor formation by activating hypoxia-inducible factor 1 (23). The present results revealed that a low concentration of SOV (0.5 μM) administered over a short period of time (24 h) stimulated 8505C cell growth; however, increases in the concentration and the treatment period inhibited 8505C cell growth in a concentration- and time-dependent manner. The IC_{50} values of SOV for 8505C growth were 3.76, 3.55, 3.23, 1.62, 0.85 and 0.80 μM on

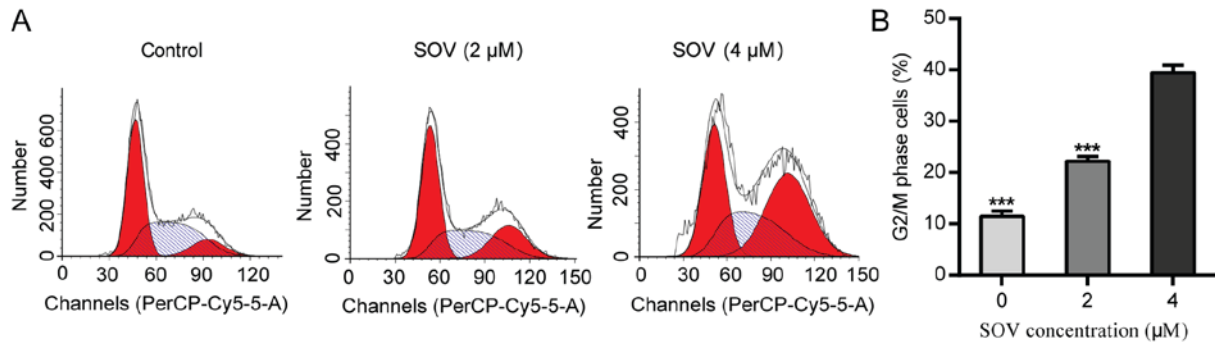


Figure 3. SOV induces G₂/M cell cycle arrest in 8505C cells. (A) DNA content and cell cycle analysis of 8505C cells treated with SOV at 0, 2 or 4 μM for 48 h. (B) Cell cycle distribution revealed that 8505C treated with SOV cells exhibited G₂/M phase arrest in a concentration-dependent manner. ***P<0.001 vs. the control (0 μM SOV) group. SOV, sodium orthovanadate.

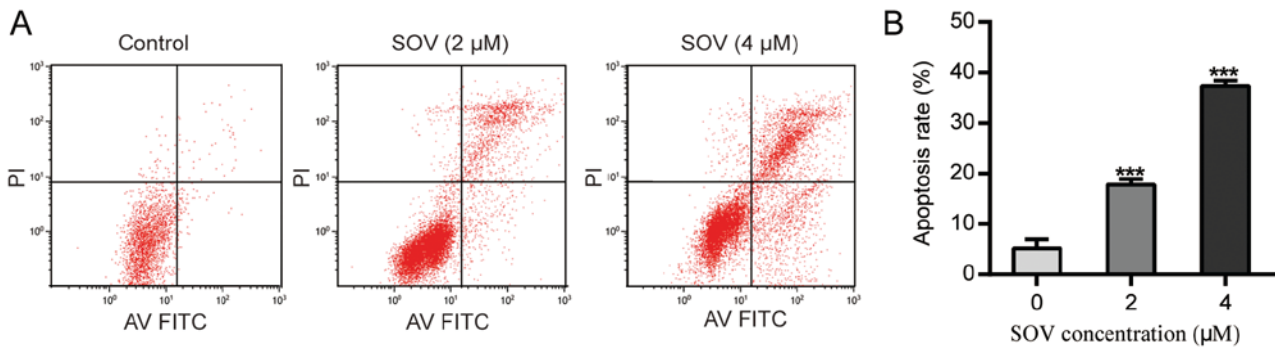


Figure 4. SOV induces apoptosis of 8505C cells. 8505C cells were treated with 0, 2 or 4 μM SOV for 48 h. (A) Flow cytometry was performed to observe apoptotic rates. (B) Representative histograms of apoptotic rates of 8505C cells. ***P<0.001 vs. the control (0 μM SOV) group. FITC, fluorescein isothiocyanate; PI, propidium iodide; SOV, sodium orthovanadate.

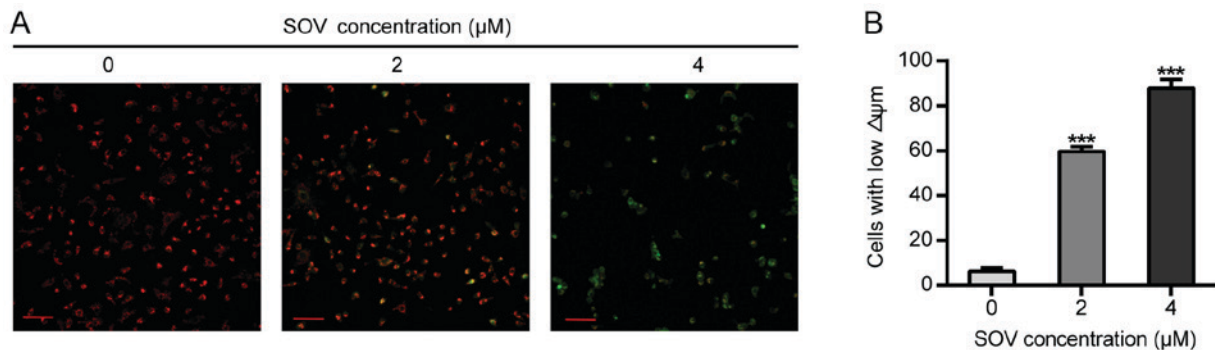


Figure 5. Alterations in $\Delta\psi_m$ of 8505C cells *in vitro*. (A) 8505C cells treated with 0, 2 or 4 μM SOV for 48 h prior to staining with JC-1. $\Delta\psi_m$ was detected by fluorescence microscopy. When $\Delta\psi_m$ was high, JC-1 accumulated in the mitochondrial matrix as a polymer (J-aggregates), producing red fluorescence; when $\Delta\psi_m$ was low, JC-1 accumulated in the mitochondrial matrix as JC-1 monomers (monomer), producing green fluorescence. (B) Representative histograms of 8505C cell labeling with JC-1 dye. Scale bar, 100 μm. ***P<0.001 vs. the control (0 μM SOV) group. SOV, sodium orthovanadate; $\Delta\psi_m$, mitochondrial membrane potential.

days 1-6, respectively. In addition, Kordowiak *et al* indicated that vanadium salts at low concentrations (0.5-1 μM) improve the morphology and viability of H35-19 rat hepatoma cells, whereas higher concentrations (2.5 μM) of vanadium act as a cellular growth inhibitor (18). In addition to cell growth, cell clone formation also decreased with increasing concentration. In the present study, SOV had a dual effect on 8505C cells: Low concentrations may promote cell growth and high concentrations inhibited tumor cell growth. This area requires further

investigation, and lower SOV concentrations and treatments duration should be tested.

Induction of cell cycle arrest can inhibit cell growth. In the present study, SOV induced tumor cell cycle arrest, resulting in the majority of cells being arrested in the G₂/M phase. Liu *et al* reported that vanadium salts induce G₂/M-phase arrest by reactive oxygen species-mediated degradation of cell division cycle 25C in PC-3 cells (15). Wu *et al* reported that vanadium salts increase the phosphorylation of cyclin B1 at

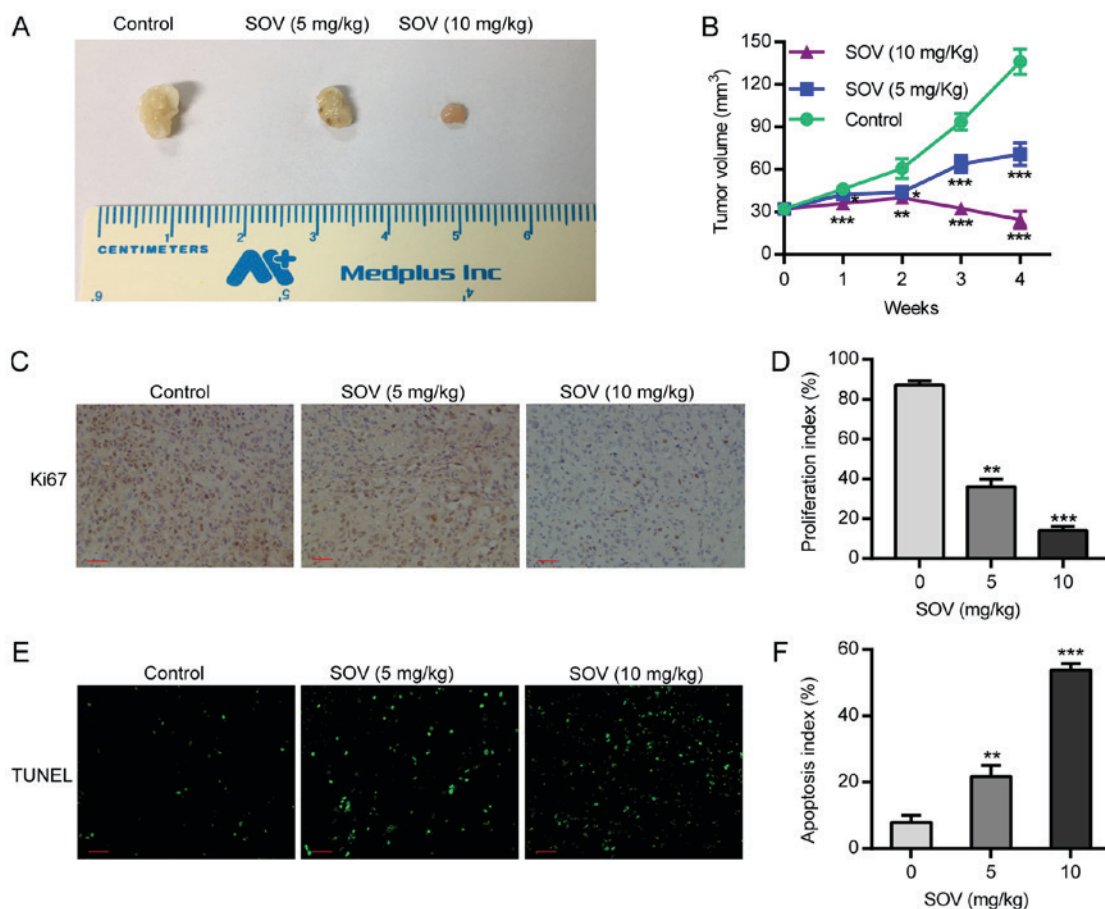


Figure 6. SOV inhibits tumor growth and induces apoptosis *in vivo*. An aliquot of 1×10^6 8505C cells was injected subcutaneously into the flanks of female nude NU/NU mice; when tumors grew to ~ 4 mm diameter, animals were randomly divided into three groups and treated with 5, 10 mg/kg SOV, or PBS. After 4 weeks of treatment, tumors were harvested. (A) 8505C xenograft tumor volumes in the different groups. (B) Alterations in 8505C xenograft tumor volume over the 4-week treatment period. (C and D) Tumor sections were stained with an anti-Ki-67 antibody to detect proliferating cells. (E and F) Tumor sections were stained with TUNEL agent to visualize apoptotic cells. Scale bar, $50 \mu\text{m}$. * $P < 0.05$, ** $P < 0.01$, *** $P < 0.001$ vs. the control (PBS) group. SOV, sodium orthovanadate; TUNEL, terminal deoxynucleotidyl transferase dUTP nick end labeling.

Thr161 and reduce its phosphorylation at Tyr15, leading to G_2/M phase arrest in HepG2, SK-Hep-1 and Hep3B cells (17). Nevertheless, Zhang *et al* reported that vanadate is also able to induce S phase arrest via p53- and p21-dependent pathways (24). In the present study, SOV induced 8505C cell cycle arrest in the G_2/M phase in a concentration-dependent manner. Treatment with $4 \mu\text{M}$ SOV resulted in the accumulation of 40% of cells in G_2/M phase, whereas only 10% of cells in the control group were in G_2/M phase.

Apoptosis induction is one of the main effects of antitumor drugs. Numerous studies have demonstrated that vanadium salts can regulate apoptosis in different ways. They can suppress (25), enhance (26–28) or induce (29) apoptosis. Morita *et al* revealed that SOV inhibits p53-mediated apoptosis (30), whereas Günther *et al* reported that SOV potentiates apoptosis induction, possibly via a p53-independent mechanism (16). In addition to p53, apoptosis is closely associated with protein levels of B-cell lymphoma 2 (Bcl-2) and Bcl-extra large (Bcl-xl) (16). Bcl-2 is located in mitochondrial membranes and endoplasmic reticulum, and regulates apoptosis. The present study demonstrated that SOV induced apoptosis of 8505C cells in a concentration-dependent manner. In addition, SOV reduced $\Delta\psi_m$ of 8505C cells, which suggested that SOV induced cell apoptosis via the mitochondrial pathway (31).

Animal models are essential for studying the effects of chemotherapeutic drugs, as their effects on complex systems, including host metabolism, host defense and the endocrine system, must be considered in order to evaluate their safety and efficacy (32). Previous studies have demonstrated that orthovanadate exerts significant anticancer effects on tumor-bearing mice. Günther *et al* reported that vanadium salts inhibit Ehrlich ascites carcinoma proliferation and enhance mice survival, and observed that vanadium combined with ascorbate at a pharmacological dose has an even better anticancer effect (16). Wu *et al* demonstrated that SOV treatment results in a clear suppression of tumor growth in a mouse orthotopic transplantation model of hepatocellular carcinoma (17). In addition, it has been indicated that vanadium administration suppresses colon carcinogenesis in rats (33). The antitumor effects of SOV on ATC xenografts *in vivo* were investigated in the present study. The results exhibited that SOV markedly suppressed tumor growth in mice xenograft models of 8505C cells. In addition, tumor growth inhibition was stronger at higher SOV concentrations (10 mg/kg) than at lower concentrations (5 mg/kg). Furthermore, via the detection of the biomarker Ki-67, results revealed that SOV significantly inhibited tumor proliferation, and TUNEL assays indicated that SOV also significantly induced tumor cell apoptosis.

A previous study has revealed that SOV acts as an antitumor agent and promotes cell death by inhibiting autophagy (17). To the best of our knowledge, the antitumor mechanism of SOV is currently not well understood, and mostly involves protein phosphatase inhibition and increases in phosphodiesterase and protein kinase activity, which are involved in cell growth and development, DNA damage, regulation of genes and proteins, and oxidative stress.

The present study has some limitations. It was not possible to elucidate the underlying mechanism of the antitumor effects of SOV, and the expression of apoptosis-associated proteins induced by cell cycle arrest were not assessed. Furthermore, the state of and changes in p53 in 8505C cells were not detected in the pathogenesis of apoptosis. Subsequently, the association between SOV-induced apoptosis and SOV-induced p53 regulation was not investigated. Finally, no attempt was made to elucidate the reason why low concentrations of SOV promoted 8505C cell growth. It may therefore be important to further investigate this point by decreasing duration and concentration of SOV treatment.

In conclusion, the present study revealed that SOV had some important anticancer effects in ATC, including the inhibition of tumor cell viability, induction of G₂/M cell cycle arrest and promotion of apoptosis. These results provided a basis for further investigations on the development of novel SOV-based chemotherapeutic drugs for the treatment of undifferentiated thyroid cancer.

Acknowledgements

The authors would like to thank Dr Shangha Pan (Central Laboratory, The First Affiliated Hospital of Harbin Medical University, Harbin, China) for his assistance with the experiments.

Funding

This study was supported by the China Medical Board (grant no. 08-894).

Availability of data and materials

The datasets used and/or analyzed during the current study are available from the corresponding author on reasonable request.

Authors' contributions

QY, HJ and WD conceived and designed the study. QY, WJ, DL, MG, KL, and LD performed the experiments. CW and QY analyzed the data. QY wrote the manuscript.

Ethics approval and consent to participate

All surgical procedures and animal care protocols were approved by the Ethics Committee of the First Affiliated Hospital of Harbin Medical University (Harbin, China).

Patient consent for publication

Not applicable.

Competing interests

The authors declare that they have no competing interests.

References

- Nagaiah G, Hossain A, Mooney CJ, Parmentier J and Remick SC: Anaplastic thyroid cancer: A review of epidemiology, pathogenesis, and treatment. *J Oncol* 2011; 542358, 2011.
- Davies L and Welch HG: Increasing incidence of thyroid cancer in the United States, 1973-2002. *Jama* 295: 2164-2167, 2006.
- Cornett WR, Sharma AK, Day TA, Richardson MS, Hoda RS, van Heerden JA and Fernandes JK: Anaplastic thyroid carcinoma: An overview. *Curr Oncol Rep* 9: 152-158, 2007.
- O'Neill JP, O'Neill B, Condrón C, Walsh M and Bouchier-Hayes D: Anaplastic (undifferentiated) thyroid cancer: Improved insight and therapeutic strategy into a highly aggressive disease. *J Laryngol Otol* 119: 585-591, 2005.
- Paunovic IR, Sipetic SB, Zoric GV, Diklic AD, Savic DV, Marinkovic J and Zivaljevic VR: Survival and prognostic factors of anaplastic thyroid carcinoma. *Acta Chir Belg* 115: 62-72, 2015.
- Perri F, Lorenzo GD, Scarpati GD and Buonerba C: Anaplastic thyroid carcinoma: A comprehensive review of current and future therapeutic options. *World J Clin Oncol* 2: 150-157, 2011.
- Kim SH, Kang JG, Kim CS, Ihm SH, Choi MG, Yoo HJ and Lee SJ: Apigenin induces c-Myc-mediated apoptosis in FRO anaplastic thyroid carcinoma cells. *Mol Cell Endocrinol* 369: 130-139, 2013.
- Yu XM, Jaskulasztul R, Ahmed K, Harrison AD, Kunnimalaiyaan M and Chen H: **Resveratrol induces differentiation markers expression in anaplastic thyroid carcinoma via activation of Notch1 signaling and suppresses cell growth.** *Mol Cancer Ther* 12: 1276-1287, 2013.
- Che H, Guo H, Si X, You Q and Lou W: Additive effect by combination of Akt inhibitor, MK-2206, and PDGFR inhibitor, tyrphostin AG 1296, in suppressing anaplastic thyroid carcinoma cell viability and motility. *Onco Ther* 7: 425-432, 2014.
- Reeb AN, Li W, Sewell W, Marlow LA, Tun HW, Smallridge RC, Copland JA, Spradling K, Chernock R and Lin RY: S100A8 is a novel therapeutic target for anaplastic thyroid carcinoma. *J Clin Endocrinol Metab* 100: 232-242, 2015.
- Alonso A, Sasin J, Bottini N, Friedberg I, Friedberg I, Osterman A, Godzik A, Hunter T, Dixon J and Mustelin T: Protein tyrosine phosphatases in the human genome. *Cell* 117: 699-711, 2004.
- Korbecki J, Baranowska-Bosiacka I, Gutowska I and Chlubek D: Biochemical and medical importance of vanadium compounds. *Acta Biochim Pol* 59: 195-200, 2012.
- Tian X, Fan J, Hou W, Bai S, Ao Q and Tong H: Sodium orthovanadate induces the apoptosis of SH-SY5Y cells by inhibiting PIWIL2. *Mol Med Rep* 13: 874-880, 2016.
- Klein A, Holko P, Ligeza J and Kordowiak AM: Sodium orthovanadate affects growth of some human epithelial cancer cells (A549, HTB44, DU145). *Folia Biol (Krakow)* 56: 115-121, 2008.
- Liu TT, Liu YJ, Wang Q, Yang XG and Wang K: Reactive-oxygen-species-mediated Cdc25C degradation results in differential antiproliferative activities of vanadate, tungstate, and molybdate in the PC-3 human prostate cancer cell line. *J Biol Inorg Chem* 17: 311-320, 2012.
- Günther TM, Kwiecinski MR, Baron CC, Felipe KB, Farias MS, da Silva FO, Bucker NC, Pich CT, Ferreira EA, Wilhelm Filho D, *et al*: Sodium orthovanadate associated with pharmacological doses of ascorbate causes an increased generation of ROS in tumor cells that inhibits proliferation and triggers apoptosis. *Biochem Biophys Res Commun* 430: 883-888, 2013.
- Wu Y, Ma Y, Xu Z, Wang D, Zhao B, Pan H, Wang J, Xu D, Zhao X, Pan S, *et al*: Sodium orthovanadate inhibits growth of human hepatocellular carcinoma cells *in vitro* and *in an orthotopic model in vivo*. *Cancer Lett* 351: 108-116, 2014.
- Kordowiak AM, Klein A, Goc A and Dabros W: Comparison of the effect of VOSO₄, Na₃VO₄ and NaVO₃ on proliferation, viability and morphology of H35-19 rat hepatoma cell line. *Pol J Pathol* 58: 51-57, 2007.
- Reed LJ and Muench H: A simple method of estimating fifty percent endpoints. *Am J Hyg* 27: 1938.
- Ostrowski J, Woszczyński M, Kowalczyk P, Trzeciak L, Hennig E and Bomsztyk K: Treatment of mice with EGF and orthovanadate activates cytoplasmic and nuclear MAPK, p70S6k, and p90rsk in the liver. *J Hepatol* 32: 965-974, 2000.

21. Choi YJ, Lim SY, Woo JH, Kim YH, Kwon YK, Suh SI, Lee SH, Choi WY, Kim JG, Lee IS, *et al*: Sodium orthovanadate potentiates EGCG-induced apoptosis that is dependent on the ERK pathway. *Biochem Biophys Res Commun* 305: 176-185, 2003.
22. Afshari CA, Kodama S, Bivins HM, Willard TB, Fujiki H and Barrett JC: Induction of neoplastic progression in Syrian hamster embryo cells treated with protein phosphatase inhibitors. *Cancer Res* 53: 1777-1782, 1993.
23. Hwang JT, Lee M, Jung SN, Lee HJ, Kang I, Kim SS and Ha J: AMP-activated protein kinase activity is required for vanadate-induced hypoxia-inducible factor 1alpha expression in DU145 cells. *Carcinogenesis* 25: 2497, 2004.
24. Zhang Z, Huang C, Li J and Shi X: Vanadate-induced cell growth arrest is p53-dependent through activation of p21 in C141 cells. *J Inorg Biochem* 89: 142-148, 2002.
25. Morita A, Zhu J, Suzuki N, Enomoto A, Matsumoto Y, Tomita M, Suzuki T, Ohtomo K and Hosoi Y: Sodium orthovanadate suppresses DNA damage-induced caspase activation and apoptosis by inactivating p53. *Cell Death Differ* 13: 499-511, 2006.
26. Gamero AM and Lerner AC: Vanadate facilitates interferon alpha-mediated apoptosis that is dependent on the Jak/Stat pathway. *J Biol Chem* 276: 13547-13553, 2001.
27. Stewart C, Mihai R and Holly JM: Increased tyrosine kinase activity but not calcium mobilization is required for ceramide-induced apoptosis. *Exp Cell Res* 250: 329-338, 1999.
28. Guo YL, Baysal K, Kang B, Yang LJ and Williamson JR: Correlation between sustained c-Jun N-terminal protein Kinase activation and apoptosis induced by tumor necrosis factor- α in rat mesangial cells. *J Biol Chem* 273: 4027-4034, 1998.
29. Figiel I and Kaczmarek L: Orthovanadate induces cell death in rat dentate gyrus primary culture. *Neuroreport* 8: 2465-2470, 1997.
30. Morita A, Yamamoto S, Wang B, Tanaka K, Suzuki N, Aoki S, Ito A, Nanao T, Ohya S, Yoshino M, *et al*: Sodium orthovanadate inhibits p53-mediated apoptosis. *Cancer Res* 70: 257-265, 2010.
31. Cossarizza A, Franceschi C, Monti D, Salvioli S, Bellesia E, Rivabene R, Biondo L, Rainaldi G, Tinari A and Malorni W: Protective effect of N-acetylcysteine in tumor necrosis factor-alpha-induced apoptosis in U937 cells: **The role of mitochondria**. *Exp Cell Res* 220: 232-240, 1995.
32. Ray RS, Ghosh B, Rana A and Chatterjee M: Suppression of cell proliferation, induction of apoptosis and cell cycle arrest: Chemopreventive activity of vanadium in vivo and in vitro. *Int J Cancer* 120: 13-23, 2007.
33. Kanna P, Mahendrakumar CB, Chakraborty T, Hemalatha P, Banerjee P and Chatterjee M: Effect of vanadium on colonic aberrant crypt loci induced in rats by 1,2 dimethyl hydrazine. *World J Gastroenterol* 9: 1020-1027, 2003.



This work is licensed under a Creative Commons Attribution-NonCommercial-NoDerivatives 4.0 International (CC BY-NC-ND 4.0) License.